

# Preliminary study on the yield of $^{225}\text{Ac}$ produced by 35 MeV @ 2 mA electron accelerator\*

Guangxin Shang,<sup>1</sup> Jiangfeng Wan,<sup>1,†</sup> Jijun Zou,<sup>1</sup> Bin Tang,<sup>1</sup> Xiangting Meng,<sup>1</sup> Yiyuan Wu,<sup>1</sup> and Zebin Lin<sup>1</sup>

<sup>1</sup>Key Laboratory of Nuclear Physics and Technology,  
East China University of Technology, Jiangxi Nanchang 330013, China

Targeted alpha therapy, as a shining new star in the field of nuclear medicine, is showing great potential in the treatment of metastatic diseases with its unique advantages.  $^{225}\text{Ac}$ , as an important  $\gamma$ -emitting medical radionuclide, its current production of less than 1.7 Ci/year restricts its development and widespread application. Therefore, exploring and optimizing the production method of  $^{225}\text{Ac}$  to increase its yield is crucial. Using a 35 MeV @ 2 mA electron accelerator to bombard a converter target produces a large number of photons. Through the photonuclear reaction  $^{226}\text{Ra}(\gamma, n)^{225}\text{Ra}$ ,  $^{225}\text{Ra}$  is generated, which can then undergo beta decay to produce  $^{225}\text{Ac}$ . Two kinds of isotope target, namely the solid plate radium target ("solid target" for short) and the solution radium target ("solution target" for short), were designed according to the special structure of the neutron source target station in this study. Under each kind of target, three target schemes, namely the internal target, the backend target and the U-shaped target were proposed. The FLUKA program was used to investigate the influence of both geometric and irradiation parameters of isotope and converter targets on the yield of  $^{225}\text{Ac}$ . The study shows that, the production capability of  $^{225}\text{Ac}$  is stronger with a solid target than with a solution target, and the  $^{225}\text{Ac}$  production capability of both solid and liquid targets is directly proportional to the irradiation time. In the internal target scheme, with a radium target containing 1.0 g of  $^{226}\text{Ra}$  and an irradiation time of 10 days, it is estimated that a 35 MeV @ 2 mA electron accelerator has an annual production capacity of 117.3 Ci of  $^{225}\text{Ac}$  when using a solid target and 12.32 Ci when using a solution target. The results indicate that bombarding radium targets with an electron accelerator enables large-scale production of  $^{225}\text{Ac}$ , ensuring a stable isotope supply for medical, research, and other applications.

Keywords: targeted alpha therapy;  $^{225}\text{Ac}$ ; solid target; solution target; electron accelerator; yield.

## I. INTRODUCTION

### A. Targeted $\alpha$ therapy and medical isotopes $^{225}\text{Ac}$

Modern medicine has driven the rapid advancement of nuclear medicine, particularly in radiodiagnosis and radiotherapy. These cutting-edge techniques for tumor diagnosis and treatment are known for their simplicity, sensitivity, accuracy, safety, and effectiveness[1–7]. Targeted alpha therapy (TAT) is a novel cancer treatment method, where a drug containing short-lived  $\alpha$ -emitting radionuclides is injected into the body. The  $\alpha$  particles emitted by the drug selectively irradiate and destroy cancer cells, achieving therapeutic goals. This therapy is characterized by its high precision, significant efficacy, and relatively minimal side effects. The production of radiopharmaceuticals for targeted  $\alpha$  therapy is an active field of academic and commercial research worldwide and is still in the development phase. Several candidate isotopes are currently undergoing clinical and preclinical evaluation,

including  $^{149}\text{Tb}$ ,  $^{211}\text{At}$ ,  $^{212}\text{Bi}$ ,  $^{212}\text{Pb}$ ,  $^{213}\text{Bi}$ ,  $^{223}\text{Ra}$ ,  $^{224}\text{Ra}$ ,  $^{227}\text{Th}$  and  $^{225}\text{Ac}$ .  $^{225}\text{Ac}$  is a highly promising  $\alpha$ -emitting radionuclide, offering several advantages: 1) The relatively short half-life of  $^{225}\text{Ac}$  (9.9 days) enhances therapeutic effectiveness while minimizing side effects. 2) It possesses favorable physicochemical properties, enabling effective binding with a variety of chelating agents. 3) Through four  $\alpha$  and two  $\beta$  decays, it ultimately transforms into stable radionuclide  $^{209}\text{Bi}$ . 4)  $^{225}\text{Ac}$  can also be used as a generator for  $^{213}\text{Bi}$  ( $T_{1/2} = 45.6$  min), which is itself a promising TAT (Targeted Alpha Therapy) isotope. 5) The energies of the  $\alpha$  particles emitted during the decays process are 5.6 MeV, 6.1 MeV, 7.1 MeV, and 5.9 MeV, totaling 24.7 MeV[8, 9]. These alpha particles can efficiently kill tumor cells while minimizing damage to surrounding healthy tissue.

### B. $^{225}\text{Ac}$ production route

The current yield of less than 1.7 Ci/year ( $6.3 \times 10^{10}$  Bq) significantly limits its potential applications in clinical practice[10], while large-scale production of  $^{225}\text{Ac}$  presents considerable challenges. Currently, the technical routes for producing  $^{225}\text{Ac}$  in academia and industry mainly include: (1) production using thorium actinide generators; (2) production using high-energy proton reactions with thorium targets; (3) production through low-energy proton reactions with radium targets; (4) production via photonuclear reactions with radium targets; (5) production through fast reactor and neutron source[10–15].

\* 1. The key project of the Open Fund supported by the Engineering Research Center of the Ministry of Education for Nuclear Technology Application at East China University of Technology, "Numerical Simulation of Target Station Physics and Target Design" (No.NHJSJYB2021-1); 2. The Youth Fund Project supported by the National Natural Science Foundation of China, "Formation mechanism and optimization research on the quasi turbulent flow zone of the gravity driven Dense Granular-flow Target in Accelerator Driven Subcritical System" (No.12205043); 3. The Jiangxi Provincial Key Research and Development Plan "Revealing the List and Commanding" Project, "Research on Key Technologies of the High-power Electron Accelerator White Neutron Source Target Station System" (No.20223BBH80005).

† Corresponding author, Jiangfeng Wan, wanjf@ecut.edu.cn

### 1. Production using thorium-actinide generators

The natural decay of  $^{229}\text{Th}$  ( $T_{1/2}=7880$  years) is currently the primary source of unsupported  $^{225}\text{Ac}$ . Every two months, up to 85 percent of the total  $^{225}\text{Ac}$  and its parent nuclide  $^{225}\text{Ra}$  can be extracted from thorium-actinium generators. Using extraction chromatography, the two are separated to obtain  $^{225}\text{Ac}$ [16].  $^{229}\text{Th}$  is primarily produced via the decay of  $^{233}\text{U}$ , but its production is limited due to the potential application of  $^{233}\text{U}$  in nuclear weapons and its high production cost. The annual effective yield of  $^{229}\text{Th}$  is only around 350 mCi (Oak Ridge National Laboratory, ORNL producing approximately 150 mCi, the Institute for Transuranium Elements, ITU producing about 46 mCi, and the Institute for Physics and Power Engineering, IPPE producing around 150 mCi[17]). Therefore, although the thorium-actinium generator provides a relatively straightforward method for producing  $^{225}\text{Ac}$ , the yield is restricted. Currently, only ORNL (annual yield of approximately 720 mCi), IPPE ( $^{229}\text{Th}$  production amount comparable to ORNL while  $^{225}\text{Ac}$  production is less certain), and ITU (annual yield of around 350 mCi) supply  $^{225}\text{Ac}$  to the market, with a total annual supply not exceeding 1.7 Ci[18–20].

### 2. Production using high-energy proton reactions with thorium targets

Using high-energy protons (proton beam energy exceeding 70 MeV) generated by accelerators can be used to bombard  $^{232}\text{Th}$  targets to produce  $^{225}\text{Ac}$ . The main advantage of this method is the easy availability of  $^{232}\text{Th}$  as a target material. However, currently only a few accelerators worldwide are capable of providing proton beams above 70 MeV. There are two primary technical approaches in this route: the first is the direct production of  $^{225}\text{Ac}$  via the  $^{232}\text{Th}(p, x)^{225}\text{Ac}$  reaction, and the second is the indirect production via the  $^{232}\text{Th}(p, x)^{225}\text{Ra} \rightarrow ^{225}\text{Ac}$  pathway. Presently, institutions such as Tri-Lab (BNL, ORNL, LANL), TRIUMF (Tri-University Meson Facility), the Institute of Nuclear Research (INR), Accelerator for Research in Radiochemistry and Oncology at Nantes Atlantique (Arronax), Isotope Decay-At-Rest (IsoDAR), the Institute of Modern Physics of the Chinese Academy of Sciences, the China Institute of Atomic Energy, have adopted these approaches[21, 22]. During high-energy proton irradiation of thorium targets, highly complex spallation reactions occur, producing hundreds of different impurity nuclides. Among these, the long-lived and toxic nuclide  $^{227}\text{Ac}$  ( $T_{1/2}=21.8$  years) constitutes approximately 0.1 percent to 0.3 percent of the total activity of  $^{225}\text{Ac}$ [23]. Since  $^{225}\text{Ac}$  and  $^{227}\text{Ac}$  are isotopes, they cannot be separated chemically, significantly limiting the large-scale production of  $^{225}\text{Ac}$ .

### 3. Production through low-energy proton reactions with radium targets

Using accelerators to produce  $^{225}\text{Ac}$  by bombarding  $^{226}\text{Ra}$  targets with medium- and low-energy protons follows the nuclear reaction  $^{226}\text{Ra}(p, 2n)^{225}\text{Ac}$ . This reaction has a relatively high cross section of 0.7 barn (at a proton energy of approximately 15.9 MeV[5, 24]). This method was first experimentally demonstrated by Apostolidis and his colleagues in 2005, showing that when the proton energy is 16.8 MeV, the yield of  $^{225}\text{Ac}$  is substantial[17]. By irradiating 30.1 mg of  $^{226}\text{Ra}$  with a 15.9 MeV @ 50  $\mu\text{A}$  proton beam for 45.3 hours, a yield of 484.7 MBq (13.1 Ci) of  $^{225}\text{Ac}$  was achieved, demonstrating the feasibility of large-scale  $^{225}\text{Ac}$  production. Currently, Germany's ITM company is collaborating with the Canadian Nuclear Laboratories (CNL) to develop this production route, with an estimated yield of 5–6 Ci per year. Additionally, the Chinese company New Radiomedicine Technology is actively developing  $^{225}\text{Ac}$  production based on this method.

### 4. Production via photonuclear reactions with radium targets

Using an accelerator producing medium or high energy electrons to bombard a heavy metal converter target can generate a large number of photons. These photons interact with a  $^{226}\text{Ra}$  target to produce  $^{225}\text{Ac}$  through the nuclear reaction  $^{226}\text{Ra}(\gamma, n)^{225}\text{Ra} \rightarrow ^{225}\text{Ac}$ . The photon energy threshold for the photonuclear reaction producing  $^{225}\text{Ra}$  is 6.4 MeV[8]. In 2005, Maslov and his colleagues first confirmed the feasibility of this method[25]. In simulations by Diamond and his colleagues, an electron beam with 20 kW power irradiating 1.0 g of  $^{226}\text{Ra}$  in a radium target for 10 days could produce 148 GBq (4 Ci) of  $^{225}\text{Ra}$ . Currently, the American company NorthStar, in collaboration with Germany's Eckert Ziegler, as well as the Belgian Nuclear Research Center SCK-CEN in partnership with IBA (Ion Beam Applications), are developing this production route. However, the photonuclear reaction route using radium targets to produce  $^{225}\text{Ac}$  still faces challenges, including the limited availability of  $^{226}\text{Ra}$  as a raw material and radiation protection for radon gas[26–29].

### 5. Production through fast reactor and neutron source

In addition to the above production methods, Japan is actively developing alternative  $^{225}\text{Ac}$  production technologies. The Japan Atomic Energy Agency (JAEA) has proposed a method based on the Joyo fast reactor, using the reaction  $^{226}\text{Ra}(\mu-, nv)^{225}\text{Fr} \rightarrow ^{225}\text{Ac}$ , as well as a method based on an accelerator neutron source through the reaction  $^{226}\text{Ra}(n, 2n)^{225}\text{Ra} \rightarrow ^{225}\text{Ac}$ . However, there are still certain issues that exist, such as the difficulty in separating  $^{225}\text{Ac}$  from various radioactive isotopes,  $^{226}\text{Ra}$  materials are difficult to obtain, radiation protection for radon gas, and hardware issues with reactors and accelerator neutron sources. In the Joyo fast reactor, irradiation generates numerous impurity nuclides in the

radium target. To obtain high-purity  $^{225}\text{Ac}$  from the radium target, in the experimental comparison among DGA resin, Ln resin, and  $\text{MnO}_2$  resin, choosing to use DGA resin for the purification process of  $^{225}\text{Ac}$  can obtain high purity of  $^{225}\text{Ac}$ [30–32]. However, fast reactors and high-flux accelerator neutron sources are extremely limited resources globally, making large-scale supply unlikely in the short term[33, 34].

### C. Research objective

According to Matyskin’s report, the current demand for  $^{225}\text{Ac}$  is approximately 185 GBq (5 Ci) per year; however, this demand is likely to be significantly affected by supply constraints and costs[12]. At 2019, there are at least 27 types of  $^{225}\text{Ac}$ -labeled molecules under development globally, with 13 having entered clinical trial phases. In the past several years, significant advancements have been made in the development of  $^{225}\text{Ac}$  labeled pharmaceuticals for various cancers, central nervous system ailments, and different infections. As a result, the number of labeled molecules reaches 73 at 2023[35, 36]. The Chinese company New Radiomedicine Technology expect  $^{225}\text{Ac}$  drugs to be commercialized by 2028, the demand for  $^{225}\text{Ac}$  will reach 100-200 Ci/year, and between 2029 and 2032, it is expected to increase to 300-500 Ci/year. As one of the most prominent  $\alpha$ -emitting radionuclides,  $^{225}\text{Ac}$  has a wide range of applications. However, with the increasing demand, providing a stable supply of  $^{225}\text{Ac}$  isotopes for medical and research applications has become urgent.

In China, East China University of Technology is establishing a white-light neutron source, called East China Accelerator Neutron Source(ECANS), which is driven by a 35 MeV @ 2 mA electron accelerator. In terms of scientific research, the facility will be used to measure neutron cross-section data and conduct neutron-related studies. In terms of applications, it can produce isotopes through photonuclear reactions, such as the medical isotopes  $^{225}\text{Ac}$ ,  $^{67}\text{Cu}$ , and  $^{47}\text{Sc}$ , such as This study utilized the photonuclear reaction of a radium target to produce  $^{225}\text{Ac}$  and conducted simulation calculations based on the FLUKA 4-4.0 and ENDF-VIII.0 databases. The relevant research results provide reference for target design in the route of photonuclear reaction producing of  $^{225}\text{Ac}$ .

## II. METHODOLOGY

### A. Methodology and Parameters

Electrons are accelerated by a 35 MeV @ 2 mA accelerator, bombarding a tungsten converter target whose total thickness is 6.0 cm in (ECANS). As a result, a large number of photons are generated through bremsstrahlung. Based on the photonuclear reaction  $^{226}\text{Ra}(\gamma, n)^{225}\text{Ra}$ ,  $^{225}\text{Ra}$  is produced, which subsequently decays to  $^{225}\text{Ac}$  via  $\beta$  decay[37, 38]. This study specifically investigates the effects of key parameters such as the spatial relationship between the isotope target and the converter target, the thickness of the converter target, the thickness of the isotope target, different target shape,  $^{226}\text{Ra}$

TABLE 1. List of parameters in solid and solution isotope target

Parameter	Value
Electron beam current	35 MeV @ 2 mA
Beam spot shape	gaussian beam spot
Beam spot FWHM	1.5 cm
Cooling water	deionized water
Irradiation time	20 hour, 120 hour, 10 day
Cooling time ( days )	0, 0.04, 0.17, 0.25, 0.33, 0.5, 0.67 0.83, 1.0, 2.0, 3.0, 6.0, 10.0, 15.0, 20
Mass of Ra target( g )	1.0, 5.0, 10.0

mass in radium target and the irradiation time in the solid and solution isotope target on the yield of  $^{225}\text{Ac}$ . Additionally, it analyzes the time-dependent activity of the impurity nuclide generated after the end of irradiation. The specific parameters studied are listed in Table 1.

### B. Solid target

When the isotope target is solid, this study designed three production target schemes for  $^{225}\text{Ac}$  medical isotopes: the internal target, the backend target, and the U-shaped target. In the internal target structure, the radium target is located behind the three tungsten converter target plates, with both the converter and radium targets situated within the same target chamber, as shown in Figure 1A. In the backend target structure, the radium target is positioned at the back (back target), the bottom (bottom target), and the side (side target) of the chamber housing the three tungsten converter targets, as illustrated in Figure 1B. In the U-shaped target structure, the radium target can be placed at the back, bottom, and side outside the chamber of the eleven tungsten converter targets, individually referred to as the back target, bottom target, and side target. The bottom and side targets are arranged in a U-shape around the sides and bottom of the converter targets, as depicted in Figure 1C.

The solid radium target sample unit is shown in Figure 2. The outer layer is an Al container with a diameter of 2.0 cm, and the internal layer is the radium target, where pure  $^{226}\text{Ra}$  is filled. In this study, the mass of the radium target is 1.0 g, and it is a cylinder with a diameter of 1.0 cm. When the radium target is a single piece, its thickness is 0.232 cm. When divided into two pieces, each has a thickness of 0.116 cm. When divided into four pieces, each has a thickness of 0.0508 cm.

### C. Solution target

When the isotope target is in solution form, the target scheme is basically the same as that of the solid target. A solid target is encased in an Al container; however, during the photon bombardment of the radium target, a large amount of heat is released, and aluminum can easily react with water at high temperatures. In contrast, S316 stainless steel has excellent corrosion resistance in high-temperature water envi-

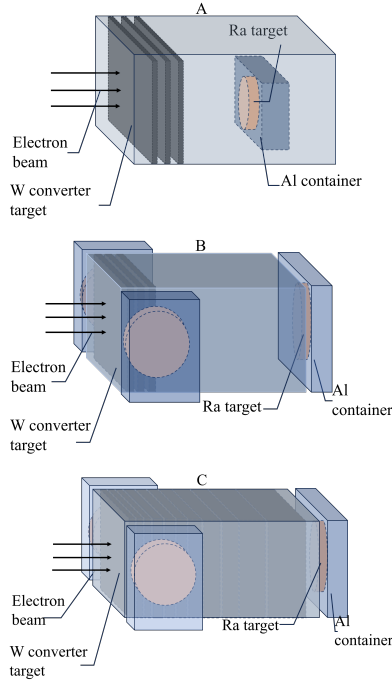


Fig. 1. Schematic diagram of the internal target (1A), the backend target (1B), and the U-shaped target (1C) of solid targets

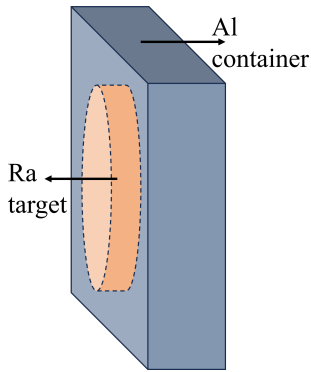


Fig. 2. Schematic diagram of solid radium target sample unit

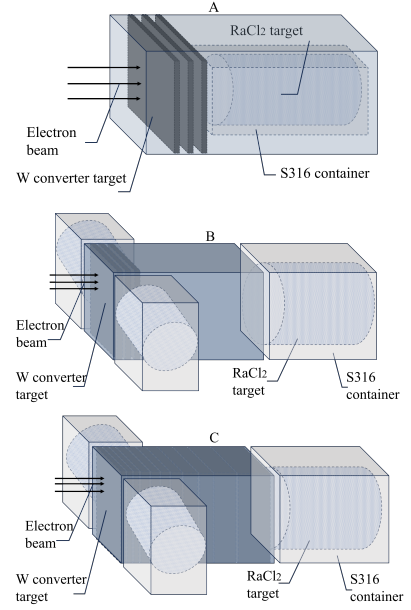


Fig. 3. Schematic diagram of the internal target (3A), the backend target (3B), and the U-shaped target (3C) of solution targets

The solution radium target sample unit is shown in Figure 4. In the isotope target, the mass of  $^{226}\text{Ra}$  are 1.0 g, 5.0 g, and 10.0 g. The outer layer is an S316 container with a diameter of 7.0 cm, while the internal layer uses  $\text{RaCl}_2$  solution as the isotope target material. When the  $\text{RaCl}_2$  solution shapes a cylindrical target, its diameter is 5.0 cm and thickness is 8.0 cm. When the  $\text{RaCl}_2$  solution shapes a cuboid target, the length, width, and height are 7.0 cm, 7.0 cm, and 3.2 cm.

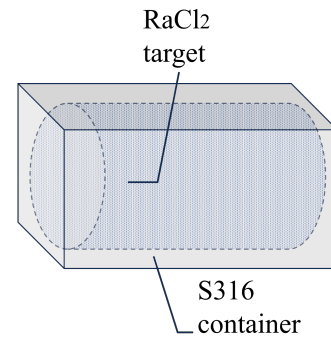


Fig. 4. Schematic diagram of solution radium target sample unit

### III. RESULTS AND DISCUSSIONS

#### A. Solid target

As shown in Figure 5, when the radium target is a single piece and irradiated for 20 hours, the activity of  $^{225}\text{Ac}$  in the internal target, backend target, and U-shaped target continues to increase during the cooling period from 0 to 15 days. From

ronments, so a solution target is encased in an S316 container. Solution target are shown in Figure 3A, B, C.



day 15 to day 20, the activity slightly decreases. On the 20th day, the total activity of  $^{225}\text{Ac}$  in the internal target, backend target, and U-shaped target reaches  $6.64 \times 10^9$  Bq,  $9.10 \times 10^8$  Bq, and  $2.65 \times 10^7$  Bq, respectively. In the backend target scheme, the yield of  $^{225}\text{Ac}$  in the back target is  $8.83 \times 10^8$  Bq, which is higher than that in the side target ( $1.28 \times 10^7$  Bq) and the bottom target ( $1.39 \times 10^7$  Bq), with the yields of the side and bottom targets being similar. In the U-shaped target scheme, the yield in the back target is the lowest at  $7.00 \times 10^6$  Bq, while the yields in the bottom target ( $1.04 \times 10^7$  Bq) and side target ( $9.14 \times 10^6$  Bq) are comparable.

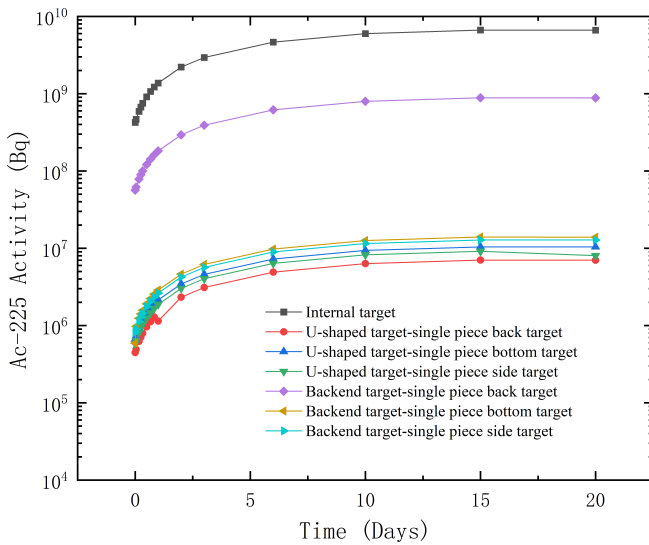


Fig. 5. Yields of  $^{225}\text{Ac}$  in different target scheme when the  $^{226}\text{Ra}$  mass in the solid target is 1.0 g.

As shown in Figure 6, when the radium target is in a single piece and irradiated for 20 hours, the activity of  $^{225}\text{Ra}$  in the internal target, backend target, and U-shaped target continuously decreases as the cooling time increases (0-20 days). On the 20th day, the total activity of  $^{225}\text{Ra}$  in the internal target, backend target, and U-shaped target reaches  $5.87 \times 10^9$  Bq,  $8.05 \times 10^8$  Bq, and  $2.44 \times 10^7$  Bq. In the backend target, the yield of  $^{225}\text{Ra}$  in the back target is  $7.80 \times 10^8$  Bq, which is much higher than that in the side target ( $1.18 \times 10^7$  Bq) and the bottom target ( $1.27 \times 10^7$  Bq), with the yields of the side and bottom targets being similar. In the U-shaped target, the yield of  $^{225}\text{Ra}$  in the back target is the lowest at ( $6.19 \times 10^6$  Bq), while the yields in the bottom target ( $9.07 \times 10^6$  Bq) and side target ( $9.09 \times 10^6$  Bq) are comparable. Since the yield of  $^{225}\text{Ac}$  in the back target is much higher than that in the side and bottom target, this kind of scheme is called the backend target scheme.

Based on Figures 5 and 6, the three target scheme for producing  $^{225}\text{Ac}$  have varying capabilities: the internal target > the backend target > the U-shaped target. In the internal target, the radium target is closest to the converter target, maximizing photon utilization and yielding the highest production. In the back target, photons are emitted perpendicularly to the target direction, resulting in a higher yield for the back target than

for the side and bottom targets. In the U-shaped target, the radium target position is similar to that of the backend target, but with the 11 tungsten converter target plates inside the chamber, affecting photon emitting from the back direction. The yield of the side and bottom targets is close and slightly higher than that of the back target.

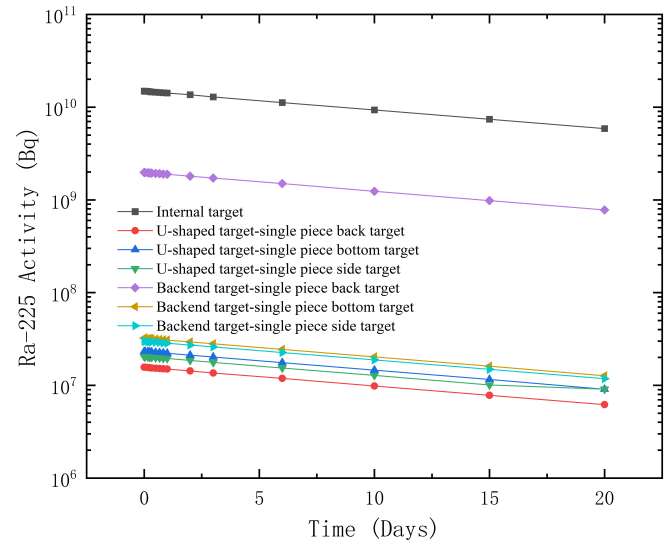


Fig. 6. Yields of  $^{225}\text{Ra}$  in different target scheme when the  $^{226}\text{Ra}$  mass in the solution target is 1.0 g.

As shown in Figure 7, when the radium target is a single piece and irradiated for 20 hours, with a cooling time of 0 to 20 days, the  $^{225}\text{Ac}$  activity varies with different tungsten converter target thicknesses. Among these,  $^{225}\text{Ac}$  yield is highest when the irradiation time is 20 hours, and the thickness of one piece tungsten converter target is 1.0 mm. The  $^{225}\text{Ac}$  activity tends to stabilize within the cooling period of 15 to 20 days.

For high-value targets such as radium, it is necessary to use a converter target before the isotope target to optimize yield. Analyzing the converter target to determine the optimal thickness is crucial for maximizing the effectiveness of the radium target.

As shown in Figure 8, in the internal target and backend target schemes with four pieces of radium targets and each radium target thickness is 0.0508 cm, while the irradiation time is 20 hours and cooling time from 0 to 15 days, the activity of  $^{225}\text{Ac}$  continuously increases in all pieces of radium target. During the 15 to 20-day period, the activity slightly decreases. The closer the distance between the single radium target and the tungsten converter target, the higher the  $^{225}\text{Ac}$  yield.

As shown in Figure 9, in the internal target scheme, when the irradiation time is 20 hours and thickness of one piece of the radium target is 0.0508 cm, the thinner the radium target, the lower the total activity of  $^{225}\text{Ac}$ . This indicates that dividing the radium target into multiple pieces of equal mass will reduce the total yield of  $^{225}\text{Ac}$ .

Based on Figures 8 and 9, the use of thin targets leads to a significant reduction in yield compared to the use of a

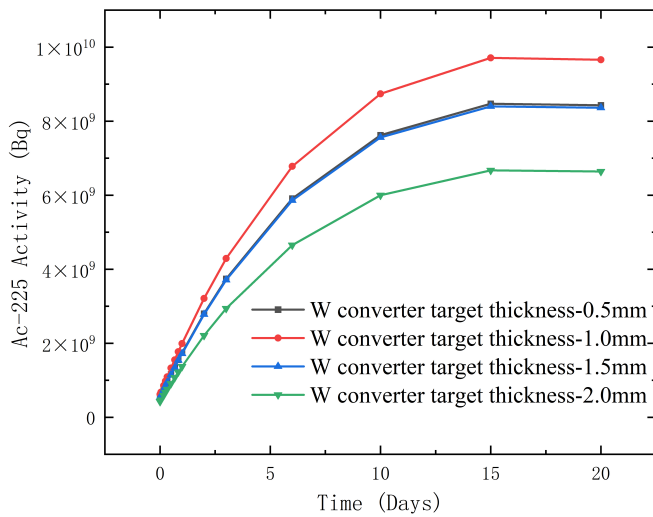


Fig. 7. Yield of  $^{225}\text{Ac}$  for different tungsten converter target thicknesses in the backend target scheme using solid target

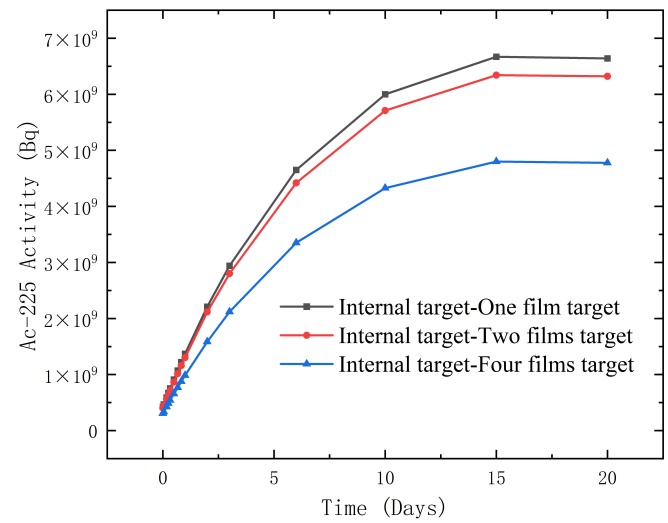


Fig. 9. Yield of  $^{225}\text{Ac}$  after 20 hours of irradiation with solid targets of different thicknesses in the internal target scheme

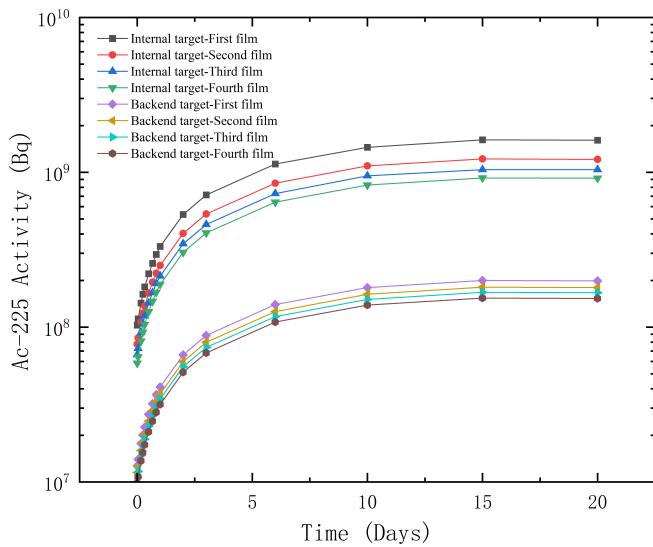


Fig. 8. Yield of  $^{225}\text{Ac}$  with different thicknesses of solid target in the film and internal target scheme

is approximately proportional to the irradiation time.

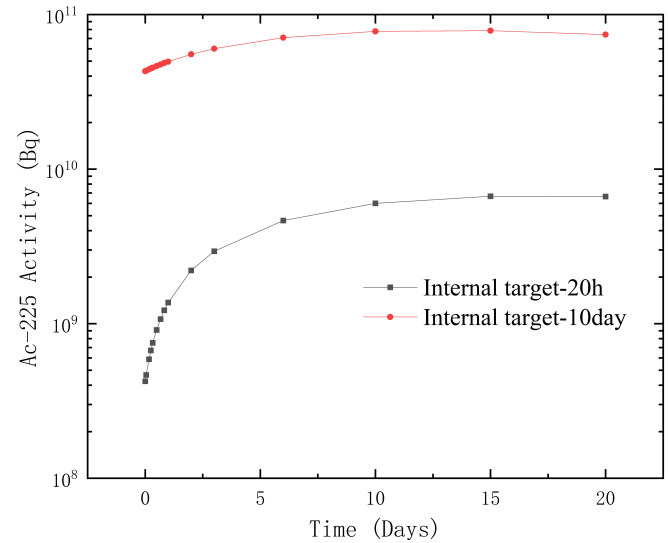


Fig. 10. Yields of  $^{225}\text{Ac}$  with irradiation times of 20 h, and 10 days in the internal target scheme when the  $^{226}\text{Ra}$  mass in the solid target is 1.0 g

thick target. However, dividing the radium target into multiple pieces allows for better heat exchange. Each piece of radium target is encapsulated in an aluminum shell, providing excellent protection for the target material. The high-power electron beam can easily penetrate both the water layer and the aluminum layer, which is consistent with the research findings of Melville G. and others.

As shown in Figure 10, in the internal target scheme, when the radium target is a single piece, the total  $^{225}\text{Ac}$  activity for an irradiation time of 10 days is much higher than that for an irradiation time of 20 hours. After cooling for 15 days, the  $^{225}\text{Ac}$  yield reaches its peak. Irradiation for 20 hours and 10 days can respectively produce  $6.67 \times 10^9$  Bq (0.18 Ci) of  $^{225}\text{Ac}$  and  $7.86 \times 10^{10}$  Bq (2.12 Ci) of  $^{225}\text{Ac}$ . The  $^{225}\text{Ac}$  yield

As shown in Figure 11, in the internal target scheme, when a single radium target is irradiated for 10 days, multiple nuclides such as  $^{225}\text{Ac}$ ,  $^{225}\text{Ra}$ ,  $^{224}\text{Ra}$ ,  $^{212}\text{Pb}$ , and  $^{212}\text{Bi}$  are produced simultaneously in the internal target. As the cooling time increases (from 0 to 20 days), the activities of  $^{225}\text{Ra}$ ,  $^{224}\text{Ra}$ ,  $^{212}\text{Pb}$ , and  $^{212}\text{Bi}$  decrease, while the activity of  $^{225}\text{Ac}$  continues to increase during the 0 to 15-day period, with a slight decrease from 15 to 20 days. At the end of irradiation, the yields of  $^{225}\text{Ra}$ ,  $^{224}\text{Ra}$ ,  $^{212}\text{Pb}$ , and  $^{212}\text{Bi}$  are  $1.45 \times 10^{11}$  Bq (3.91 Ci),  $1.92 \times 10^{11}$  Bq (5.19 Ci),  $1.87 \times 10^{11}$  Bq (5.05 Ci), and  $1.87 \times 10^{11}$  Bq (5.05 Ci), respectively. Regarding the

separation and extraction of  $^{225}\text{Ac}$ , the research findings of Diamond W.T. et al. suggest that the first separation should be carried out 15 days after the end of beam irradiation, followed by additional separations every 15 days. If each extraction is 100 percent efficient, the total  $^{225}\text{Ac}$  activity extracted over three consecutive separations would approach the total activity of  $^{225}\text{Ra}$  at the end of irradiation. This indicates that, in the internal target scheme, the maximum activity of  $^{225}\text{Ac}$  that can be extracted from the radium target irradiated for 10 days' irradiation is  $1.45 \times 10^{11}$  Bq (3.91 Ci), which corresponds to the amount of  $^{225}\text{Ra}$  immediately after irradiation is completed. If the electron accelerator operates for an effective irradiation time of 300 days per year, approximately 117.3 Ci of  $^{225}\text{Ac}$  can be produced annually.

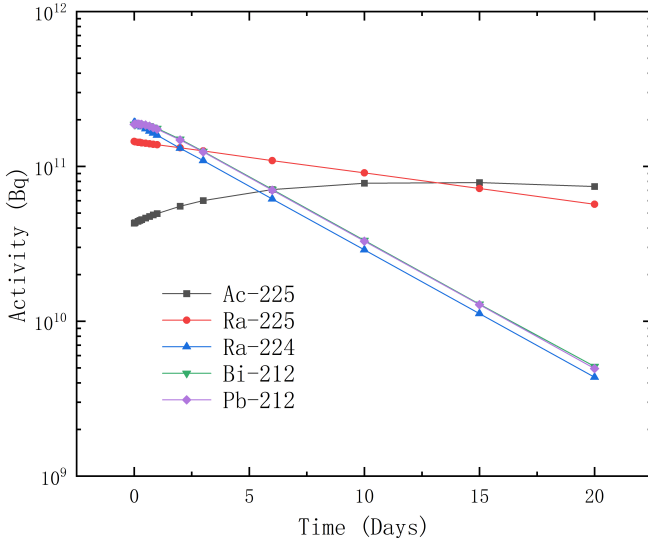


Fig. 11. The production of various isotopes in the internal target scheme after 10 days of irradiation in the solid target

### B. Solution target

In the internal target scheme, when the  $^{226}\text{Ra}$  mass in the radium target is 1.0 g, 5.0 g, and 10.0 g respectively, the yields of  $^{225}\text{Ra}$  and  $^{225}\text{Ac}$  at the end of beam irradiation are shown in Table 2. The yields of  $^{225}\text{Ra}$  and  $^{225}\text{Ac}$  are approximately proportional to the mass of  $^{226}\text{Ra}$  in the radium target.

TABLE 2. Irradiation for 10 days, yields of  $^{225}\text{Ra}$  and  $^{225}\text{Ac}$  with different  $^{226}\text{Ra}$  mass in a solution target

$^{226}\text{Ra}$ Different mass (g)	$^{225}\text{Ra}$ Yield (Ci)	$^{225}\text{Ac}$ Yield (Ci)
1.0	0.411	0.122
5.0	2.062	0.614
10.0	4.270	1.270

As shown in Figure 12, when the  $^{226}\text{Ra}$  mass in the radium target is 1.0 g, after 10 days of irradiation, the activity of  $^{225}\text{Ac}$  in the internal target, backend target, and U-shaped

target continues to increase during a cooling period of 0 to 15 days. From 15 to 20 days, the activity slightly decreases. On the 20th day, the total activity of  $^{225}\text{Ac}$  in the internal target, backend target, and U-shaped target reaches  $7.81 \times 10^9$  Bq,  $3.22 \times 10^9$  Bq, and  $7.71 \times 10^7$  Bq. In the U-shaped target scheme, the yield of the backend target is the lowest at  $2.20 \times 10^7$  Bq, while the yields of the bottom target and side target are comparable at  $3.10 \times 10^7$  Bq and  $2.41 \times 10^7$  Bq.

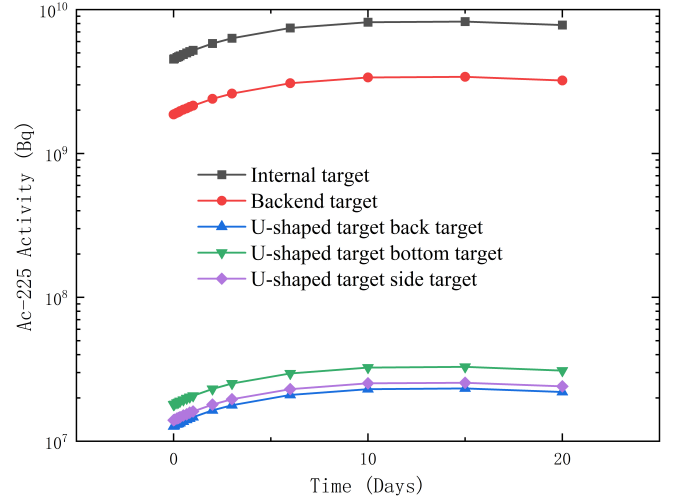


Fig. 12. Yields of  $^{225}\text{Ac}$  in different target scheme when the  $^{226}\text{Ra}$  mass in the solution target is 1.0 g

As shown in Figure 13, when the  $^{226}\text{Ra}$  mass in the radium target is 1.0 g, after 10 days of irradiation, the activity of  $^{225}\text{Ra}$  in the internal target, backend target, and U-shaped target decreases continuously with increasing cooling time (0–20 days). On the 20th day, the total activity of  $^{225}\text{Ra}$  in the internal target, backend target, and U-shaped target reaches  $6.00 \times 10^{10}$  Bq,  $2.47 \times 10^9$  Bq, and  $5.92 \times 10^7$  Bq. In the U-shaped target, the yield of  $^{225}\text{Ra}$  in the backend target is the lowest at  $1.69 \times 10^7$  Bq, while the yields of the bottom target and side target are comparable at  $2.38 \times 10^7$  Bq and  $1.85 \times 10^7$  Bq. The production capacities of the three target configurations are similar to those of a solid target.

As shown in Figure 14, in the backend target scheme, when the  $^{226}\text{Ra}$  mass in the radium target is 1.0 g and irradiated for 10 days, the  $^{225}\text{Ac}$  activity varies with different isotopic target shapes. During the cooling period from 0 to 15 days, the  $^{225}\text{Ac}$  activity in the cylindrical and rectangular targets continues to increase, reaching  $1.87 \times 10^9$  Bq and  $1.50 \times 10^9$  Bq at the end of irradiation, respectively. From 15 to 20 days, the activity slightly decreases, and on the 20th day, the activity reaches  $3.22 \times 10^9$  Bq for the cylindrical target and  $2.59 \times 10^9$  Bq for the rectangular target. The cylindrical target is more effective in producing  $^{225}\text{Ac}$  than the rectangular target.

As shown in Figure 15, in the internal target scheme, when the  $^{226}\text{Ra}$  mass in the radium target is 1.0 g and the irradiation time is 10 days, the total activity of  $^{225}\text{Ac}$  is slightly higher than that at 120 hours of irradiation and significantly higher than that at 20 hours. After a 15-day cooling period, the yield

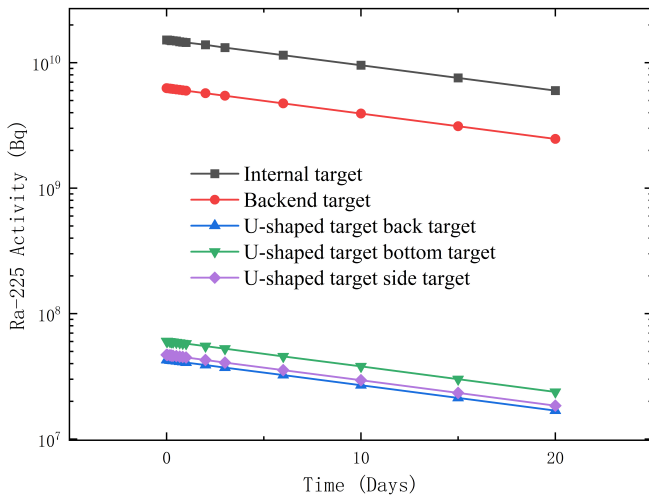


Fig. 13. Yields of  $^{225}\text{Ra}$  in different target scheme when the  $^{226}\text{Ra}$  mass in the solution target is 1.0 g

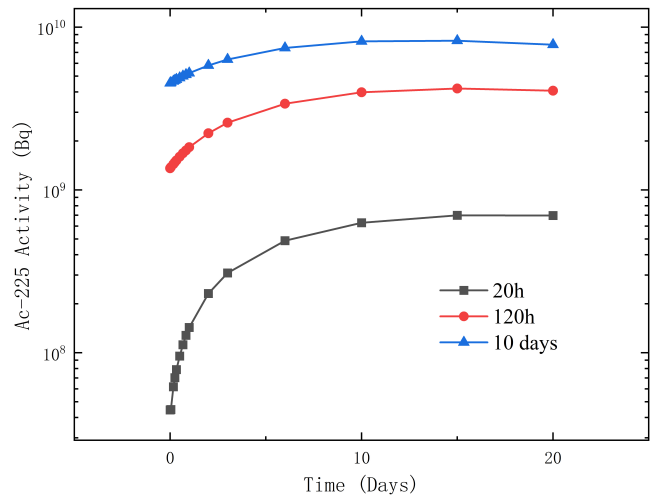


Fig. 15. Yields of  $^{225}\text{Ac}$  with irradiation times of 20 h, 120 h, and 10 days in the internal target scheme when the  $^{226}\text{Ra}$  mass in the solution target is 1.0 g

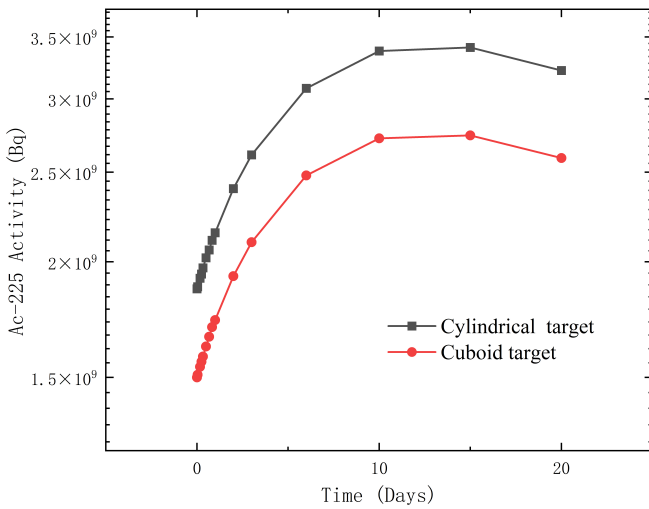


Fig. 14. Yields of  $^{225}\text{Ac}$  in different solution target shapes when the  $^{226}\text{Ra}$  mass in the solution target is 1.0 g

of  $^{225}\text{Ac}$  reaches its peak and then stabilizes between 15 and 20 days. Irradiation times of 20 hours, 120 hours, and 10 days yield  $6.96 \times 10^8$  Bq,  $4.07 \times 10^9$  Bq, and  $7.81 \times 10^9$  Bq of  $^{225}\text{Ac}$ , respectively, with yields approximately proportional to irradiation time.

As shown in Figure 16, in the internal target scheme, when the  $^{226}\text{Ra}$  mass in the radium target is 1.0 g, various radionuclides such as  $^{225}\text{Ac}$ ,  $^{225}\text{Ra}$ ,  $^{224}\text{Ra}$ ,  $^{221}\text{Fr}$ ,  $^{220}\text{Rn}$ ,  $^{212}\text{Pb}$ , and  $^{212}\text{Bi}$  are present in the internal target. As the cooling time increases (0 to 20 days), the activities of  $^{225}\text{Ra}$ ,  $^{224}\text{Ra}$ ,  $^{220}\text{Rn}$ ,  $^{212}\text{Pb}$ , and  $^{212}\text{Bi}$  decrease, while the activities of  $^{225}\text{Ac}$  and  $^{221}\text{Fr}$  continue to increase between 0 and 15 days. Between 15 and 20 days, the activity of  $^{225}\text{Ac}$  and  $^{221}\text{Fr}$  slightly decreases. At the end of irradiation, the yields of  $^{225}\text{Ac}$ ,  $^{225}\text{Ra}$ ,  $^{224}\text{Ra}$ ,  $^{221}\text{Fr}$ ,  $^{220}\text{Rn}$ ,  $^{212}\text{Pb}$ , and  $^{212}\text{Bi}$  are  $4.53 \times 10^9$  Bq,  $1.52 \times 10^{10}$  Bq,  $1.91 \times 10^{10}$  Bq,  $1.37 \times 10^7$  Bq,  $2.55 \times 10^7$  Bq,  $1.86 \times 10^{10}$  Bq, and  $1.86 \times 10^{10}$  Bq, respectively. If the extraction scheme is the same as that used for solid targets, after three extractions, the maximum theoretical activity of  $^{225}\text{Ac}$  that can be extracted from the radium target after 10 days of irradiation is  $1.52 \times 10^{10}$  Bq (0.411 Ci). If the electron accelerator has an effective irradiation time of 300 days per year, approximately 12.32 Ci of  $^{225}\text{Ac}$  can be produced.

Bq,  $1.91 \times 10^{10}$  Bq,  $1.37 \times 10^7$  Bq,  $2.55 \times 10^7$  Bq,  $1.86 \times 10^{10}$  Bq, and  $1.86 \times 10^{10}$  Bq, respectively. If the extraction scheme is the same as that used for solid targets, after three extractions, the maximum theoretical activity of  $^{225}\text{Ac}$  that can be extracted from the radium target after 10 days of irradiation is  $1.52 \times 10^{10}$  Bq (0.411 Ci). If the electron accelerator has an effective irradiation time of 300 days per year, approximately 12.32 Ci of  $^{225}\text{Ac}$  can be produced.

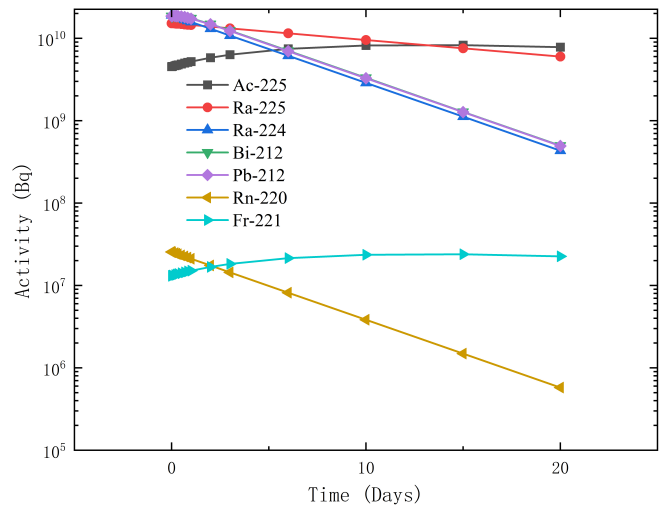


Fig. 16. The production of various isotopes in the internal target scheme after 10 days of irradiation in the solution target



## C. Discussion

### 1. Data comparison and target design

As shown in Table 3, the production capacity of the solid target for producing  $^{225}\text{Ac}$  is superior to that of the solution target. When the  $^{226}\text{Ra}$  mass in the radium target is 1.0 g and the irradiation time is 10 days, the production  $^{225}\text{Ac}$  by the solid target under internal target scheme is approximately ten times that of the solution target, showing the largest discrepancy. The U-shaped target scheme follows, with the solid target producing approximately four times the amount of  $^{225}\text{Ac}$  compared to the solution target. The backend target scheme has the smallest discrepancy, where the solid target produces approximately three times the amount of  $^{225}\text{Ac}$  as the solution target.

The  $^{225}\text{Ac}$  production capability of both solid and solution targets is directly proportional to the irradiation time. In the internal target scheme, with 1.0 g of  $^{226}\text{Ra}$  and a cooling time of 15 days, the solid target produces  $^{225}\text{Ac}$  at yields of  $6.67 \times 10^9$  Bq (0.18 Ci) and  $7.86 \times 10^{10}$  Bq (2.12 Ci) for irradiation times of 20 hours and 10 days. Under the same conditions, the solution target produces  $^{225}\text{Ac}$  at  $6.96 \times 10^8$  Bq (0.02 Ci) and  $7.81 \times 10^9$  Bq (0.21 Ci). With irradiation times of 20 hours and 10 days, the multiplicative relationship between the yields of the solid target and the solution target is generally consistent with the multiplicative relationship between the irradiation times.

When selecting the radium target state and scheme, the following factors should also be considered, 1) When choosing between a solid target or a solution target, the target preparation process, cost and yield should be considered. The target preparation process for solid targets is complex, solid targets are may prepared by electroplating, which is costly and technically complex, but the yield is high. When using solid targets, high temperatures may cause the radium target to melt, making heat dissipation particularly important. For solution targets,  $^{226}\text{Ra}$  is usually dissolved in an acidic solution. Solution target preparation process is simpler, facilitates subsequent separation and purification, and aids in managing the main decay product of  $^{226}\text{Ra}$ ,  $^{222}\text{Rn}$ , but the overall yield is lower. 2) When selecting among the three target types, the difficulty of target chamber design, cost, and yield should be taken into consideration. For the internal target, the radium target and tungsten converter target are located within the same chamber, although this configuration yields higher production, it makes target replacement difficult and increases engineering complexity and cost. In contrast, the U-shaped target, though lower in yield, places the radium target outside the converter target chamber, making the design simpler and target replacement easier. The choice of target design should be based on practical considerations.

### 2. Radon processing

As one of the nuclides in the decay chain of  $^{226}\text{Ra}$ ,  $^{220}\text{Rn}$  and their decay products release  $\alpha$  particles during the de-

cay process, which can damage the human airway and lungs; Among the decay products of  $^{220}\text{Rn}$ ,  $^{210}\text{Po}$  is extremely toxic, Weight for weight,  $^{210}\text{Po}$  is about  $2.50 \times 10^{11}$  times more toxic than hydrocyanic acid, the lethal dose for an adult male weighing 70 kg is around 0.7 micrograms, although it produces almost no lethal dose in natural radiation, attention should still be paid. According to assessments by the World Health Organization (WHO) and the International Agency for Research on Cancer (IARC), the International Commission on Radiological Protection (ICRP) recommends that indoor radon concentration should be kept below  $100 \text{ Bq/m}^3$ , while the International Atomic Energy Agency (IAEA) sets a reference level of  $300 \text{ Bq/m}^3$  for basic safety standards. A 1.0 g radium target, through radioactive decay, can produce  $3.65 \times 10^{10}$  Bq  $^{222}\text{Rn}$  per second. Although the amount of  $^{222}\text{Rn}$  generated through photonuclear in radium targets the almost negligible ( $9.08 \times 10^4$  Bq), the quantity of  $^{222}\text{Rn}$  remains far above acceptable levels, protection against  $^{222}\text{Rn}$  is a challenge. radon removal methods typically rely on its physical adsorption properties.

In Rickard et al.'s patent, highly porous structure activated carbon is applied in the solution target system to adsorb radon gas, thereby reducing the concentration of radon. The advantage of this method is its ability to effectively treat radon gas in smaller spaces, and through the adsorption capacity of activated carbon, it reduces the long-term accumulation risks of radon in the environment. Solid targets still need further exploration.

## IV. CONCLUSION

In this study, 35 MeV @ 2 mA electron was used to bombard a tungsten converter target, producing a large number of photons through bremsstrahlung. Based on the photonuclear reaction  $^{226}\text{Ra}(\gamma, n)^{225}\text{Ra}$ ,  $^{225}\text{Ra}$  was generated, which subsequently decays to  $^{225}\text{Ac}$  via  $\beta$  decay. The production yields of  $^{225}\text{Ra}$  and  $^{225}\text{Ac}$  in radium targets of different states were specifically studied across the three target configurations, leading to the following conclusions:

1. The production capability of  $^{225}\text{Ac}$  is stronger with a solid target than with a solution target. For a radium target containing 1.0 g of  $^{226}\text{Ra}$  and irradiated for 10 days, the maximum yields of  $^{225}\text{Ac}$  using the internal, backend, and U-shaped target scheme for the solid target are 3918.92 mCi, 524.32 mCi, and 15.76 mCi. In comparison, the maximum yields for the solution target are 419.81 mCi, 169.45 mCi, and 4.06 mCi.

2. The  $^{225}\text{Ac}$  production capability of both solid and solution targets is directly proportional to the irradiation time. In the internal target scheme, with 1.0 g of  $^{226}\text{Ra}$  and a cooling time of 15 days, the solid target produces  $^{225}\text{Ac}$  at yields of  $6.67 \times 10^9$  Bq (0.18 Ci) and  $7.86 \times 10^{10}$  Bq (2.12 Ci) for irradiation times of 20 hours and 10 days. Under the same conditions, the solution target produces  $^{225}\text{Ac}$  at  $6.96 \times 10^8$  Bq (0.02 Ci) and  $7.81 \times 10^9$  Bq (0.21 Ci).

3. For the solid target, 1) in the internal target scheme, the highest  $^{225}\text{Ac}$  yield is achieved with a tungsten converter

target thickness of 1.0 mm, reaching  $9.66 \times 10^9$  Bq (0.26 Ci) at the EOB. 2) Dividing the same mass of the isotopic target into multiple segments and positioning them closer to the converter target results in higher  $^{225}\text{Ac}$  yields, although the total yield of  $^{225}\text{Ac}$  decreases.

4. For the solution target, within the internal target scheme, 1) the yields of  $^{225}\text{Ra}$  and  $^{225}\text{Ac}$  are directly proportional to the mass of  $^{226}\text{Ra}$  in the radium target. When the  $^{226}\text{Ra}$  mass in the radium target is 1.0 g, 5.0 g, and 10.0 g, the theoretical maximum extractable yields of  $^{225}\text{Ac}$  are 0.411 Ci, 2.062 Ci, and 4.270 Ci. 2) A cylindrical target has a stronger  $^{225}\text{Ac}$  production capability than a rectangular target, with the cylindrical and rectangular targets yielding  $^{225}\text{Ac}$  at  $1.87 \times 10^9$  Bq and  $1.50 \times 10^9$  Bq.

5. For a radium target with a mass of 1.0 gram and an irradiation time of 10 days, the maximum theoretical activity of  $^{225}\text{Ac}$  that can be separated and extracted from the solid target is  $1.45 \times 10^{11}$  Bq (3.91 Ci), while for the solution target, it is  $1.52 \times 10^{10}$  Bq (0.42 Ci), which is the amount of  $^{225}\text{Ra}$ . Based on this, it is estimated that a 35 MeV @ 2 mA electron accelerator has an annual production capacity of 117.3 Ci of  $^{225}\text{Ac}$  when using a solid target and 12.32 Ci when using a

solution target.

If we want to provide a stable supply of  $^{225}\text{Ac}$ , larger radium targets are needed. However, the supply of  $^{226}\text{Ra}$  as a raw material remains challenging due to its scarcity and high cost. Additionally, the generation of impurity isotopes complicates the process of  $^{225}\text{Ac}$  separation and extraction, necessitating the development of efficient chemical separation and purification techniques to isolate  $^{225}\text{Ac}$  from numerous impurity isotopes. Overall, the insufficient production of  $^{225}\text{Ac}$  is the main obstacle limiting its potential applications. Currently, producing  $^{225}\text{Ac}$  through photonuclear reactions on radium targets is one of the promising methods to increase  $^{225}\text{Ac}$  yield. The ECANS constructed by East China University of Technology, utilizing a 35 MeV @ 2 mA electron beam to irradiate radium targets, is expected to play an important role in providing a stable supply of  $^{225}\text{Ac}$  isotopes for research and other applications in the future.

## V. BIBLIOGRAPHY

- [1] Fouad A Abolaban, Essam M Banoqitah, Eslam M Taha, Abdulsalam M Alhawsawi, Fathi A Djouider, and Andrew Nisbet. Production of actinium-225 from a (n, p) reaction: Feasibility and pre-design studies. *Nukleonika*, 66(2):61–67, 2021.
- [2] Christos Apostolidis, Roger Molinet, John McGinley, Kamel Abbas, J Möllenbeck, and Alfred Morgenstern. Cyclotron production of ac-225 for targeted alpha therapy. *Applied Radiation and Isotopes*, 62(3):383–387, 2005.
- [3] Kwamena E Baidoo, Kwon Yong, and Martin W Brechbiel. Molecular pathways: targeted  $\alpha$ -particle radiation therapy. *Clinical cancer research*, 19(3):530–537, 2013.
- [4] B Bayanov, V Belov, and S Taskaev. Neutron producing target for accelerator based neutron capture therapy. In *Journal of Physics: Conference Series*, volume 41, page 460. IOP Publishing, 2006.
- [5] Rose A Boll, Dairin Malkemus, and Saed Mirzadeh. Production of actinium-225 for alpha particle mediated radioimmunotherapy. *Applied Radiation and Isotopes*, 62(5):667–679, 2005.
- [6] Olivier Couturier, Stéphane Supiot, Marie Degraef-Mougin, Alain Faivre-Chauvet, Thomas Carlier, Jean-François Chatal, François Davodeau, and Michel Cherel. Cancer radioimmunotherapy with alpha-emitting nuclides. *European journal of nuclear medicine and molecular imaging*, 32:601–614, 2005.
- [7] WT Diamond and CK Ross. Actinium-225 production with an electron accelerator. *Journal of Applied Physics*, 129(10), 2021.
- [8] Jörgen Elgqvist, Sofia Frost, Jean-Pierre Pouget, and Per Albertsson. The potential and hurdles of targeted alpha therapy—clinical trials and beyond. *Frontiers in oncology*, 3:324, 2014.
- [9] Mohamed A Gizawy and Nader MA Mohamed. Potential production of ac-225 at egyptian second research reactor (etr-2) through neutron induced transmutation of ra-226. *Applied Radiation and Isotopes*, 205:111176, 2024.
- [10] Terry Grimm, Amanda Grimm, William Peters, and Mike Zammiara. High-purity actinium-225 production from radium-226 using a superconducting electron linac. *Journal of Medical Imaging and Radiation Sciences*, 50(1):S12–S13, 2019.
- [11] James T Harvey. Northstar perspectives for actinium-225 production at commercial scale. *Current Radiopharmaceuticals*, 11(3):180–191, 2018.
- [12] Maria Hassan, Tanveer Hussain Bokhari, Nadeem Ahmed Lodhi, Muhammad Kaleem Khosa, and Muhammad Usman. A review of recent advancements in actinium-225 labeled compounds and biomolecules for therapeutic purposes. *Chemical Biology & Drug Design*, 102(5):1276–1292, 2023.
- [13] Tatsuya Higashi, Kotaro Nagatsu, Atsushi B Tsuji, and Ming-Rong Zhang. Research and development for cyclotron production of 225ac from 226ra—the challenges in a country lacking natural resources for medical applications. *Processes*, 10(6):1215, 2022.
- [14] Eline L Hooijman, Valery Radchenko, Sui Wai Ling, Mark Konijnenberg, Tessa Brabander, Stijn LW Koolen, and Erik de Blois. Implementing ac-225 labelled radiopharmaceuticals: practical considerations and (pre-) clinical perspectives. *EJN-MMI Radiopharmacy and Chemistry*, 9(1):9, 2024.
- [15] Ji Hu, Hongyu Li, Yanying Sui, and Jin Du. Current status and future perspective of radiopharmaceuticals in china. *European Journal of Nuclear Medicine and Molecular Imaging*, 49(8):2514–2530, 2022.
- [16] Daiki Iwahashi, Yuto Sasaki, Tomoatsu Shinohara, and Naoyuki Takaki. Semi-permanent mass production of ac-225 for cancer therapy by the (3n, x) reaction in pressurized water reactor. *Processes*, 12(1):83, 2023.
- [17] Andrey G Kazakov, Taisya Y Ekatoeva, and Julia S Babenya. Photonuclear production of medical radiometals: A review of experimental studies. *Journal of Radioanalytical and Nuclear Chemistry*, 328:493–505, 2021.
- [18] Young-Seung Kim and Martin W Brechbiel. An overview of targeted alpha therapy. *Tumor biology*, 33:573–590, 2012.
- [19] AA Kotovskii, NA Nerozin, IV Prokof'ev, VV Shapovalov,

- 647 Yu A Yakovshchits, AS Bolonkin, and AV Dunin. Isolation of  
648 actinium-225 for medical purposes. *Radiochemistry*, 57:285–  
649 291, 2015.
- 650 [20] OD Maslov, AV Sabel'nikov, and SN Dmitriev. Preparation of  
651 225 ac by 226 ra ( $\gamma$ , n) photonuclear reaction on an electron  
652 accelerator, mt-25 microtron. *Radiochemistry*, 48:195–197,  
653 2006.
- 654 [21] Artem V Matyskin, Susanna B Angermeier, Saleem S Drera,  
655 Michael C Prible, Jeffrey A Geuther, and Michael D Heibel.  
656 Actinium-225 photonuclear production in nuclear reactors us-  
657 ing a mixed radium-226 and gadolinium-157 target. *Nuclear*  
658 *Medicine and Biology*, 136:108940, 2024.
- 659 [22] Daniel R McAlister and E Philip Horwitz. Characterization of  
660 extraction of chromatographic materials containing bis (2-ethyl-  
661 1-hexyl) phosphoric acid, 2-ethyl-1-hexyl (2-ethyl-1-hexyl)  
662 phosphonic acid, and bis (2, 4, 4-trimethyl-1-pentyl) phosphinic  
663 acid. *Solvent extraction and Ion exchange*, 25(6):757–769,  
664 2007.
- 665 [23] Daniel R McAlister and E Philip Horwitz. Chromatographic  
666 generator systems for the actinides and natural decay series  
667 elements. *Radiochimica Acta*, 99(3):151–159, 2011.
- 668 [24] G Melville, Sau Fan Liu, and BJ Allen. A theoretical model  
669 for the production of ac-225 for cancer therapy by photon-  
670 induced transmutation of ra-226. *Applied radiation and iso-*  
671 *topes*, 64(9):979–988, 2006.
- 672 [25] Graeme Melville and Barry J Allen. Cyclotron and linac produc-  
673 tion of ac-225. *Applied radiation and isotopes*, 67(4):549–555,  
674 2009.
- 675 [26] Alfred Morgenstern, Christos Apostolidis, and Frank Bruchert-  
676 seifer. Supply and clinical application of actinium-225 and  
677 bismuth-213. In *Seminars in nuclear medicine*, volume 50,  
678 pages 119–123. Elsevier, 2020.
- 679 [27] KL Pomykala, BA Hadaschik, O Sartor, S Gillessen,  
680 CJ Sweeney, T Maughan, MS Hofman, and K Herrmann. Next  
681 generation radiotheranostics promoting precision medicine. *An-*  
682 *nals of Oncology*, 34(6):507–519, 2023.
- 683 [28] Ali Pourmand and Nicolas Dauphas. Distribution coefficients  
684 of 60 elements on todga resin: application to ca, lu, hf, u and th  
685 isotope geochemistry. *Talanta*, 81(3):741–753, 2010.
- 686 [29] Valery Radchenko, Alfred Morgenstern, Amir R Jalilian, Cate-  
687 rina F Ramogida, Cathy Cutler, Charlotte Duchemin, Cornelia  
688 Hoeher, Ferrid Haddad, Frank Bruchertseifer, Haavar Gausemel,  
689 et al. Production and supply of  $\alpha$ -particle-emitting radionu-  
690 clides for targeted  $\alpha$ -therapy. *Journal of nuclear medicine*,  
62(11):1495–1503, 2021.
- 691 [30] Badra Sanditya Rattyanaanda, Duyeh Setiawan, Muhamad Basit  
692 Febrian, Rasito Tursinah, Rudi Gunawan, Teguh Hafiz Ambar  
693 Wibawa, Yanuar Setiadi, Isa Mahendra, and Ahmad Kurniawan.  
694 Preliminary study of radioisotopes actinium-225 (225ac) pro-  
695 duction using indonesian decy-13 cyclotron conceptual design.  
696 In *AIP Conference Proceedings*, volume 2967. AIP Publishing,  
697 2024.
- 698 [31] Andrew KH Robertson, Caterina F Ramogida, Paul Schaffer,  
699 and Valery Radchenko. Development of 225ac radiopharma-  
700 ceuticals: Triumf perspectives and experiences. *Current radio-*  
701 *pharmaceuticals*, 11(3):156–172, 2018.
- 702 [32] Yuto Sasaki and Shigetaka Maeda. Effect of 226ra purity as  
703 a target for 225ac production using a fast reactor. *Journal of*  
704 *Radioanalytical and Nuclear Chemistry*, pages 1–10, 2024.
- 705 [33] Yuto Sasaki, Aaru Sano, Shinji Sasaki, Nobuyuki Iwamoto,  
706 Kazuki Ouchi, Yoshihiro Kitatsuji, Naoyuki Takaki, and Shige-  
707 taka Maeda. Evaluation of the production amount of 225ac  
708 and its uncertainty through the 226ra (n, 2n) reaction in the  
709 experimental fast reactor joyo. *Journal of Nuclear Science and*  
710 *Technology*, 61(4):509–520, 2024.
- 711 [34] George Sgouros, Bin He, Nitya Ray, Dale L Ludwig, and Eric C  
712 Frey. Dosimetric impact of ac-227 in accelerator-produced ac-  
713 225 for alpha-emitter radiopharmaceutical therapy of patients  
714 with hematological malignancies: a pharmacokinetic modeling  
715 analysis. *EJNMMI physics*, 8:1–16, 2021.
- 716 [35] Masashi Takada, Kazuaki Kosako, Koji Oishi, Takashi  
717 Nakamura, Kouichi Sato, Takashi Kamiyama, and Yoshi-  
718 aki Kiyanagi. Angular distributions of absorbed dose of  
719 bremsstrahlung and secondary electrons induced by 18-, 28-and  
720 38-mev electron beams in thick targets. *Radiation protection*  
721 *dosimetry*, 153(3):369–383, 2013.
- 722 [36] RK Yadav and R Shanker. Energy and angular distributions  
723 of backscattered electrons from the collision of 8-kev elec-  
724 trons with a thick tungsten target. *Physical Review A—Atomic,*  
725 *Molecular, and Optical Physics*, 70(5):052901, 2004.
- 726 [37] Boris L Zhuikov. Successes and problems in the development  
727 of medical radioisotope production in russia. *Physics-Uspekhi*,  
728 59(5):481, 2016.
- 729 [38] Barbara Zielinska, Christos Apostolidis, Frank Bruchertseifer,  
730 and Alfred Morgenstern. An improved method for the produc-  
731 tion of ac-225/bi-213 from th-229 for targeted alpha therapy.  
732 *Solvent Extraction and Ion Exchange*, 25(3):339–349, 2007.